

1 Only a minority of bacteria grow after wetting in both
2 natural and post-mining biocrusts in a hyperarid,
3 phosphate mine

4
5 Talia Gabay^{1,2}, Eva Petrova³, Osnat Gillor², Yaron Ziv¹, and Roey Angel^{3*}

6
7 ¹Department of Life Sciences, Ben Gurion University of the Negev, 8410501, Israel

8 ²Zuckerberg Institute for Water Research, Blaustein Institutes for Desert Research, Ben-Gurion
9 University of the Negev, 8499000, Israel

10 ³Institute of Soil Biology and Biogeochemistry, Biology Centre CAS, Na Sádkách 7, 370 05 České
11 Budějovice, Czech Republic

12
13 Correspondence: Roey Angel (roey.angel@bc.cas.cz), Talia Gabay (taliamoann@gmail.com)

Formatted: Complex Script Font: Assistant Light

Formatted: Complex Script Font: Assistant Light

Formatted: Complex Script Font: Assistant Light

Formatted: Complex Script Font: Assistant Light

Formatted: Complex Script Font: Assistant Light

Formatted: Font: (Default) Cambria, Complex Script
Font: Cambria

Formatted: Complex Script Font: Assistant Light

Abstract

Biological soil crusts (biocrusts) are key contributors to desert ecosystem functions; therefore, biocrust restoration following mechanical disturbances is imperative. In the Negev Desert hyperarid regions, phosphate mining has been practiced for over 60 years, destroying soil habitats, and fragmenting the landscape. ~~To understand the effects of mining activity on soil health, we previously characterized the biocrust communities in four phosphate mining sites over spatial (post-mining and natural plots) and temporal (2-10 years since restoration) scales. We showed that bacterial abundance, richness, and diversity in natural plots were significantly higher than in post-mining plots, regardless of temporal scale.~~ In this study, we selected one mining site restored in 2007, and used DNA stable isotope probing (DNA-SIP) to identify which bacteria grow in post-mining and adjacent natural biocrusts. Since biocrust communities activate only after wetting, we incubated the biocrusts with H_2^{18}O for 96 hours under ambient conditions. We then evaluated the physicochemical soil properties, chlorophyll *a* concentrations, activation, and functional potential of the biocrusts. The DNA-SIP assay revealed low bacterial activity in both plot types and no significant differences in the proliferated communities' composition when comparing post-mining and natural biocrusts. We further found no significant differences in the microbial functional potential, photosynthetic rates, or soil properties. Our results suggest that growth of hyperarid biocrust bacteria after wetting is minimal. We hypothesize that due to the harsh climatic conditions, during wetting bacteria devote their meager resources to prepare for the coming drought, by focusing on damage repair, and organic compound synthesis and storage rather than on growth. These low growth rates contribute to the sluggish recovery of desert biocrusts

37 following major disturbances such as mining. Therefore, our findings highlight the need for
38 implementing active restoration practices following mining.

39



Formatted: Complex Script Font: Assistant Light

40 **Keywords**

41 Biological soil crust; Biocrust restoration; Stable isotope probing; Hyperarid desert; Mining;

42 Ecological restorationRestoration

43



Formatted: Complex Script Font: Assistant Light

44

1. Introduction

Phosphate mining in the Negev Desert, Israel, has been taking place since the 1960s in large areas. ILC-Rotem mining company leads the phosphate mining activities and has been practicing a reclamation-oriented mining protocol for the past 15 years. The mining protocol entails the excavation of the top 50-70 cm of soil (which they consider to be topsoil) followed by the overburden (the layer covering the phosphate), then storing the two soil layers in separate piles. Following the excavation of the phosphate, the overburden is returned to the mining pit followed by the topsoil. Finally, the terrain is leveled with heavy machinery. The area is then considered a restored, post-mining site.

Open mining activities lead to the destruction of the local vegetation and seed bank, and the fragmentation of the natural landscape (Sengupta, 2021). The consequences include land degradation, erosion, soil and water pollution, and dust dispersion. In addition, mining activity often leads to decreased biodiversity in and around mining sites (Bridge, 2004, Sengupta, 2021). One of the ecosystem components being destroyed by mining activities in the Negev Desert is the biological soil crust layer (biocrust). Biocrust is the topmost layer of many arid soils and comprises primary-producing and heterotrophic microorganisms that bind together soil particles using secreted extracellular polymeric substances (EPS), mainly polysaccharides (Weber et al., 2022). Biocrusts provide many ecosystem services, including fixing nitrogen and carbon, and soil stabilization (Belnap and Lange, 2003). While biocrust microorganisms developed various adaptations to withstand the harsh desert environment

Formatted: Complex Script Font: Assistant Light

66 (Makhalanyane et al., 2015), biocrust structures are susceptible to mechanical disturbances.
67 Such a disturbance, especially over large scales (for example, mining activity), breaks and
68 buries biocrust organisms, often resulting in changed biocrust communities (Belnap and
69 Eldridge, 2003).

70

71 In a previous research, we evaluated the biocrust bacterial communities in phosphate
72 mining sites (Gabay et al., 2022). Briefly, we found that natural and post-mining biocrusts
73 differ in community composition and diversity. Following the biocrust community analysis,
74 we sought to identify which bacterial groups are actively growing in the biocrust and
75 whether the composition differs between natural and post-mining sites. To this end, we used
76 DNA-stable isotope probing (DNA-SIP): a culture-free approach that allows the detection of
77 actively growing microorganisms by labeling them with stable isotopes such as ^{15}N , ^{14}C , and
78 ^{18}O (Dumont and Hernández García, 2019). SIP has been widely applied in identifying
79 microbial groups that participate in carbon and nitrogen cycling, such as methanotrophs

80 (Sultana et al., 2019, Zhang et al., 2020), methylotrophs (Macey et al., 2020, Arslan et al.,
81 2022), and nitrogen fixers (Pepe-Ranney et al., 2016, Angel et al., 2018). Likewise, SIP can use
82 the incorporation of heavy water (H_2^{18}O) into various biomarkers to study the growth and
83 function of microorganisms that become activated upon wetting (Schwartz et al., 2019).

84 Previous H_2^{18}O SIP experiments measured microbial growth rates and dynamics following
85 hydration (Blazewicz et al., 2020). Desert biocrusts make an ideal study system for H_2^{18}O SIP
86 experiments, as they become active quickly following hydration (Angel and Conrad, 2013),

Formatted: Complex Script Font: Assistant Light

Formatted: Complex Script Font: Assistant Light

Formatted: Complex Script Font: Assistant Light

Formatted: Complex Script Font: Assistant Light

Formatted: Complex Script Font: Assistant Light

Formatted: Complex Script Font: Assistant Light

Formatted: Complex Script Font: Assistant Light

87 resuming growth, nutrient cycling, and excretion of extracellular organic materials (Garcia-
88 Pichel and Belnap, 1996, Belnap and Lange, 2003).

Formatted: Complex Script Font: Assistant Light

Formatted: Complex Script Font: Assistant Light

89

90 In this research, we investigated the proliferation of bacterial groups in biocrusts taken from
91 reference ('natural') areas and post-mining sites by incubating biocrust samples with
92 isotopically-labeled water (H_2^{18}O). We hypothesized that growth patterns and taxonomic
93 identity of bacterial groups would differ significantly when comparing natural and post-
94 mining biocrusts. Specifically, we expected higher bacterial growth rates in natural
95 compared to post-mining biocrusts. Based on our previous findings, we specifically expected
96 higher activity of Cyanobacteria in the natural biocrusts (Gabay et al., 2022).

Formatted: Complex Script Font: Assistant Light

2. Materials and Methods

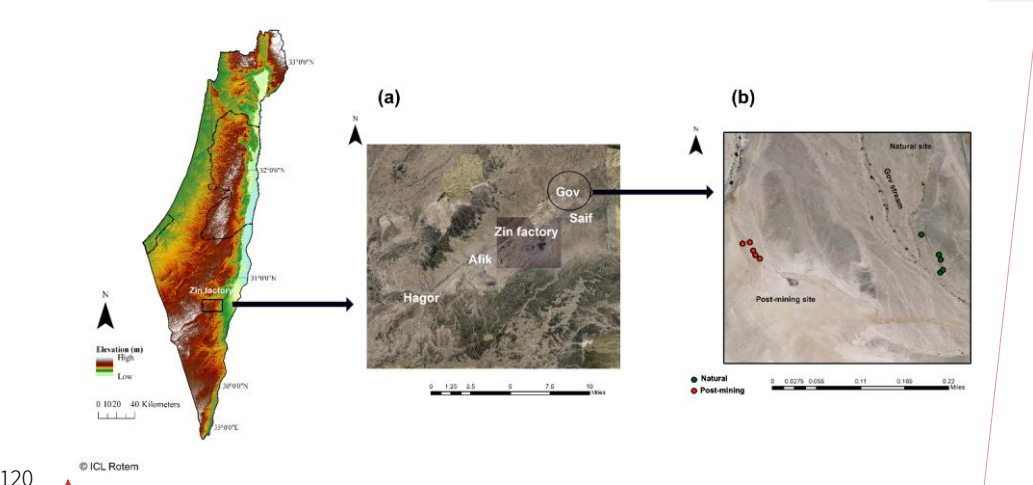
2.1. Study site and sample collection

Sampling was conducted during June 2020 at the Gov Mining Site, located in the Zin Valley (30.84 °N, 35.09 °E, 98 m above sea level), where restoration was completed in 2007. The study area was previously described in Gabay et al., (2022). Briefly, Zin Valley is a hyperarid region of the Negev Desert, with 50 mm average annual rainfall (Zin factory meteorological data). ~~The and soils are~~ highly saline soils (average EC = 24 dS/m) ~~REF~~. The main soil cover types in Zin Valley are biocrusts and desert pavement, with scarce vegetation of mainly annual species. The soil composition in the post-mining site and natural area is similar with 70% sand, 18% silt and 12% clay, REF and 68% sand, 20% silt and 12% clay REF for natural and post-mining respectively (Gabay et al., 2022). composed of variable amounts of sand, silt, and clay, and The soils in Zin Valley are classified as Solonchaks according to the World Reference Based soil classification system ~~REF~~.

Formatted: Complex Script Font: Assistant Light

Biocrusts were sampled either from the post-mining site or the adjacent natural area. The biocrusts in Gov are thin (between 1.5 - 2.5 mm deep), and smooth. The site is characterized by areas covered in biocrusts or desert pavement. In each sampling site, we sampled along a 100 m strip at approximately 10 m intervals (Fig. 1). In total, we sampled 20 biocrust samples (10 from each site). We collected the biocrusts using a spatula, at an average depth of 2 mm. Biocrusts were placed in 100 mm x 15 mm petri dishes lined with cotton. For the SIP assay, we

118 chose 5 of the 10 samples from each site containing the highest chlorophyll *a* concentrations
119 as estimated in preliminary experiments (Table S1).



120 Figure 1: map of the research area. Map a shows the different post-mining sites around the
121 Zin factory. Map b shows the biocrust sampling points in gov mining site used for this
122 research. Green dots represent the natural biocrusts, and red dots represent the post-mining
123 biocrusts.
124

127 2.2. Soil properties

128 Five biocrust samples from each plot type (post-mining and natural) were sent for analysis of
129 soil properties (pH, EC, NO_3^- concentrations, and soil organic matter). The analysis was
130 performed at the Gilat Soil Laboratory (Gilat Research Center, Gilat, Israel).

131

132 2.3. chlorophyll *a* extraction

133 Chlorophyll *a* was extracted from biocrust samples using a protocol previously described in
134 Gabay et al., (2022). Briefly, chlorophyll *a* was extracted from 3 g soil of each biocrust sample
135 was diluted in 9 mL of methanol for 15 min at 65 °C. The soil solution was centrifuged at 2000
136 rpm for 5 minutes, supernatant was collected, and absorbance was measured in a
137 spectrophotometer at 665 nm. Concentrations were calculated according to (Ritchie, 2006)
138 ~~Ritchie (2006)~~ and normalized to 1 g of soil. Extractions of the biocrusts were performed before
139 (dry biocrusts) and after 96 hr incubation with distilled water (DW) under identical conditions
140 to the incubation with H₂¹⁸O.

Formatted: Complex Script Font: Assistant Light

142 2.4. Stable isotope probing

Formatted: Complex Script Font: Assistant Light

143 2.4.1. Soil incubation

144 To test the incorporation of ¹⁸O into biocrust samples, a microcosm was designed to control
145 for the incubation conditions. Each microcosm consisted of a 10 mL glass vial in which 1 g of
146 biocrust sample was placed. To achieve field water-holding capacity, 0.15 mL of H₂¹⁸O or
147 DNase-free water were added. The glass vials were then sealed with butyl rubber stoppers
148 (Sigma-Aldrich, St. Louis, Missouri, United States) to prevent evaporation. Both labeled and
149 unlabeled controls were incubated in duplicates, for a total of 40 vials. Samples were
150 incubated under a 12 hr photoperiod for 96 hr in an incubator (FOC 225 I, VELP Scientifica,
151 Usmate Velate MB, Italy) to allow the incorporation of ¹⁸O into the bacterial DNA. Following
152 incubation, the microcosms were sacrificed, and each biocrust sample was divided into 4

153 bead beating tubes (Qiagen, Hilden, Germany), each containing 0.25 g of soil, and stored at -
154 80 °C until further analysis.

155 Each labeled sample had a non-labeled control, incubated under identical conditions but
156 with DNase-free water instead of ^{18}O water.

157

158 **2.4.2. DNA extraction**

159 DNA was extracted from all biocrust samples using DNeasy PowerSoil Pro Kit (Qiagen),
160 according to the manufacturer's instructions. The biomass in hyperarid biocrusts tends to be
161 very low, yielding only minute amounts of DNA. Therefore, each 1 g soil was extracted in
162 batches of 0.25 g, and the extracts were later consolidated to increase DNA yield.

163

164 **2.4.3. SIP gradient preparation and fractionation**

165 DNA (ca. 3.5 ng) was subjected to isopycnic gradient centrifugation in a solution of caesium
166 chloride (7.163 M; CsCl, Sigma Aldrich. St Loise, MI, USA) and buffer (0.1 M Tris-HCl at pH 8.0,
167 0.1 M KCl and 1 mM EDTA, all from Sigma Aldrich) to a final density of 1.725 g mL^{-1} as described

168 previously (Jia et al., 2019). The tubes were spun for 44 hr at 177,000 g and then fractionated
169 by water displacement using a syringe pump (NE-300 Just Infusion™ Syringe Pump, NewEra
170 Pump systems, Farmingdale, NY, USA). The refractive index was measured using an AR200
171 digital refractometer (Reichert, Depew, NY, USA) and then the DNA was precipitated using a
172 Polyethylene Glycol 6000 solution (30% PEG 8000 and 1.6 M NaCl), and 30 µg of GlycoBlue

Formatted: Complex Script Font: Assistant Light

Formatted: Complex Script Font: Assistant Light

Formatted: Complex Script Font: Assistant Light

173 Coprecipitant (Thermo Fisher Scientific, Waltham, MS, USA). Copy numbers of the 16S rRNA
174 gene in each fraction were determined by qPCR using a probe-based approach. Primers 338F
175 and 805R (Yu et al., 2005), coupled with a 516P probe (FAM-BHQ1 dual labeled) were used for
176 the assay. Per one reaction 10 µL of TaqMan™ Fast Advanced Master Mix (Thermo Fisher
177 Scientific), 0.4 µL of Bovine Saline Albumin (BSA; Thermo Fisher Scientific), 1 µL of each primer
178 (10 µM), 0.4 µL of a probe (10 µM) and 2.2 µL of PCR water was combined and mixed with 5 µL
179 of DNA. After 5 min initial denaturation at 95 °C, cycling program: 40 cycles of 95 °C for 30 sec
180 followed by 62 °C for 1 min was applied. Gene copy numbers were established from a standard
181 curve of *Escherichia coli* 16S rRNA gene.

Formatted: Complex Script Font: Assistant Light

Formatted: Complex Script Font: Assistant Light

Formatted: Complex Script Font: Assistant Light

182 183 2.4.4. PCR and sequencing

Formatted: Complex Script Font: Assistant Light

Formatted: Complex Script Font: Assistant Light

184 Following fractionation, all samples (labeled and unlabeled) were amplified using the 16S
185 rRNA primers 515F_mod and 806R_mod (Apprill et al., 2015; Parada et al., 2016). ~~Apprill et al.~~
186 ~~2015, Parada et al. 2016~~. Each reaction consisted of 2.5 µL Green Taq Buffer (Thermo Fisher
187 Scientific), 2.5 µL of dNTP set (Biotechrabbit, Berlin, Germany), 0.1 µL of BSA (Thermo Fisher
188 Scientific), 0.625 µL of each primer (10 µM), 0.125 µL DreamTaq Green DNA Polymerase
189 (Thermo Fisher Scientific) and 17.5 µL of PCR water (Sigma). The PCR ran for 38 cycles using
190 the following program: denaturation at 94 °C for 45 sec, annealing at 52 °C for 45 sec, extension
191 at 72 °C for 45 sec, and a final cycle of extension at 72 °C for 10 min. The amplified fragments
192 were sequenced using MiniSeq (Illumina, San Diego, CA, USA) at the UIC sequencing core,
193 University of Illinois, Chicago, Illinois (<https://rrc.uic.edu/cores/genome-research/genome->

Formatted: Complex Script Font: Assistant Light

194 [research-core/](#)). DNA extraction and SIP gradient controls, PCR negative controls and mock
195 community (ZymoBIOMICS Microbial Community Standard II Log Distribution; Zymo
196 Research, Irvine, CA, USA) samples (2 of each) were also sequenced to control for
197 contaminants in the sequencing results.

198 ▲

199 2.5. Bioinformatic analysis

200 All the bioinformatic and statistical analyses were done in R V4.1.1 (R development core
201 team, 2013). Labeling of bacteria was detected using differential abundance analysis as
202 described in Angel (2019). Briefly, the sequences were processed using the DADA2 package
203 V8.8 (Callahan et al., 2016) for quality filtering, denoising, read-merging, chimera removal,
204 constructing amplicon sequence variants (ASV) tables, and taxonomic assignment. Detection
205 and removal of potential contaminant sequences were performed using the R package
206 decontam V.1.12.0 (Davis et al., 2017). Prevalence filtering of rare ASVs was done using the
207 Phyloseq package V1.36.0 (McMurdie and Holmes, 2013). ASVs that appeared in less than
208 2.5% of the samples were removed. A maximum-likelihood phylogenetic tree was calculated
209 using IQ-TREE2 V 2.1.1. (Minh et al., 2020). Finally, differential abundance analysis was
210 performed using DESeq2 V1.32.0 (Love et al., 2014) to compare the relative abundance of
211 each ASV in the heavy fractions of labeled DNA to the unlabeled heavy fractions (the negative
212 control samples), which allows identifying the bacterial groups that incorporated the water
213 isotope into their DNA. The results were filtered to include only ASVs with a 2-fold log change
214 and a significance value $p < 0.1$.

Formatted: Complex Script Font: Assistant Light

Formatted: Complex Script Font: Assistant Light

Formatted: Complex Script Font: Assistant Light

215

216 2.6. Predictions of genomic functions

Formatted: Complex Script Font: Assistant Light

217 Abundances of functional genes based on 16S rRNA gene abundances were performed using
218 ~~PICRUSt2~~ Picrust2 (Douglas et al., 2019). Abundances of functional genes were predicted based
219 on a filtered ASV table containing only ASVs belonging to proliferated bacteria based on the
220 differential abundance modeling. The resulting output is functional identifications that were
221 annotated using the KEGG database to infer functional gene families. Each gene was then
222 classified into ~~10 function categories~~ a function category and ~~The the~~ abundance of genes
223 within each category was averaged. ~~based~~ The function categories were chosen based on
224 Meier et al. (2021). In their study, Meier et al. collected biocrusts from the Negev and analyzed
225 bacterial metagenomes in the biocrusts to evaluate the distribution of metabolic potential
226 among bacterial populations. To compare functional potential between various bacterial
227 phyla, they selected metabolic genes encoded in the metagenomic-assembled genomes and
228 grouped them into 10 function categories. ~~The abundance of genes within each category was~~
229 ~~averaged.~~

230

231 2.7. Statistical analyses

Formatted: Complex Script Font: Assistant Light

232 chlorophyll *a* concentrations were visualized as an estimation plot using the dabestr
233 package V0.3.0 (Ho and Tumkaya, 2018). The effect size was calculated as a bootstrap 95%
234 confidence interval. Relative abundances of phyla. Abundances of functional genes and soil
235 properties were compared between natural and post-mining biocrusts using Mann-Whitney

236 tests. The community composition of natural and post-mining biocrusts was assessed using
237 only sequences belonging to proliferated bacteria based on DESeq2 modeling. The weighted
238 UniFrac (Lozupone et al., 2011) was used to calculate the similarity between the natural and
239 post-mining communities, and an adonis model was used to assess whether communities
240 differ significantly from each other (package Vegan V2.6-2; Dixon, 2003).

Formatted: Complex Script Font: Assistant Light

241

Formatted: Complex Script Font: Assistant Light

3. Results

Sample wetting and greening

Most biocrust samples (both natural and post-mining) showed greening within 36 to 48 hr into the 96 hr incubation. By the end, most samples displayed varying degrees of greening, indicating cyanobacterial activity. Generally, post-mining biocrust showed less greening than the natural biocrusts (Fig. 2).

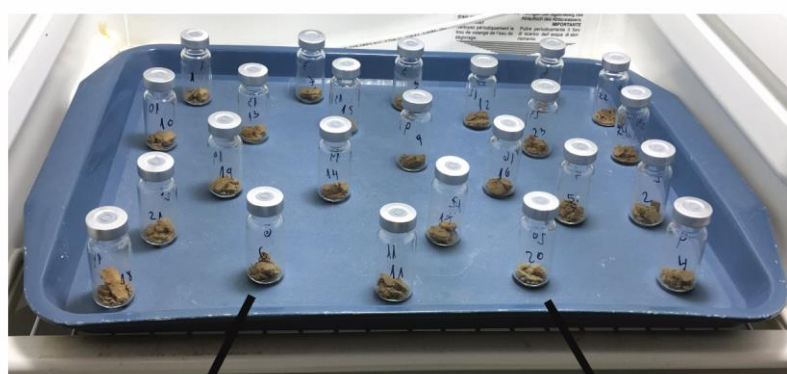


Figure 2: Incubation setup. Top picture – biocrusts in sealed glass vials in the incubator. Bottom picture – natural (a) and post-mining (b) biocrusts following the 96-hour incubation.

Formatted: Complex Script Font: Assistant Light

254 **Soil properties**

Formatted: Complex Script Font: Assistant Light

255 EC and NO₃⁻ were significantly higher in natural biocrusts compared to post-mining biocrusts
256 (EC: t = 2.89, p < 0.05; NO₃⁻: t = 4, p < 0.01; Table 1). Soil organic matter was also significantly
257 higher in the natural biocrusts (t = 3.77, p < 0.01; Table 1). pH was slightly higher in natural
258 biocrusts; however, the differences were not statistically significant (pH: t = 1.41, p = 0.19;
259 Table 1).

261 Table 1: soil properties for natural and post-mining biocrusts. The numbers represent the
262 means for each property and the standard deviation. Significant differences are marked
263 with an asterisk (* = p < 0.05; ** = p < 0.01).

264

Plot type/Soil property	Natural	Post-mining
pH	7.6 ± 0.12	7.5 ± 0.1
EC	26.22* ± 9.38	9.94 ± 8.39
NO ₃	84.82** ± 36.69	14.75 ± 13.57
Soil organic matter	1.2** ± 0.19	0.81 ± 0.12

Formatted: Font: (Default) Assistant Light, 12 pt, Complex Script Font: Assistant Light, 12 pt

Formatted: Centered

Formatted Table

Formatted: Font: (Default) Assistant Light, 12 pt, Complex Script Font: Assistant Light, 12 pt

Formatted: Font: (Default) Assistant Light, 12 pt, Complex Script Font: Assistant Light, 12 pt

Formatted: Font: (Default) Assistant Light, 12 pt, Complex Script Font: Assistant Light, 12 pt

Formatted: Font: (Default) Assistant Light, 12 pt, Complex Script Font: Assistant Light, 12 pt

265

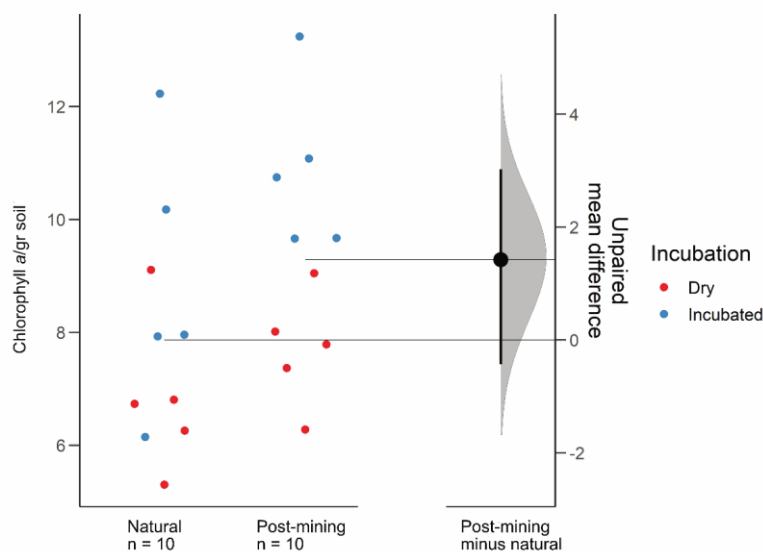
266

267 **Chlorophyll a**

Formatted: Complex Script Font: Assistant Light

268 The estimation plot revealed an effect size estimate at 1.42 (95CI -0.432; 3.03; Fig. 3). In the
269 natural samples, there was no clear clustering according to the soil water content i.e., dry or
270 hydrated (following 96 hr incubation with water). In fact, there was a larger variance between

271 samples collected after incubation (Fig. 3). Hydrated post-mining biocrusts had consistently
272 higher chlorophyll *a* concentrations compared to dry biocrusts. It is also apparent that the
273 variance between samples was smaller in the post-mining biocrusts (Fig. 3).



274 ▲ Figure 3: Estimation plots of chlorophyll *a* concentrations. Dots represent the biocrust
275 samples, and colors represent either dry or incubated soil.
276

277

278 Sequencing and differential abundance modeling

279 Sequencing resulted in 47,311 reads per sample on average (Table S2) and 10,275 ASVs
280 (Table S3). Following decontamination and filtering, 86% of the ASVs were removed (Table
281 S3). However, they accounted for only 16% of the total reads. Out of the remaining 1,404
282 ASVs, 1,266 in total were labeled and used for the differential abundance modeling (Table
283 S3). Each sequence in the labeled samples was compared to its corresponding negative

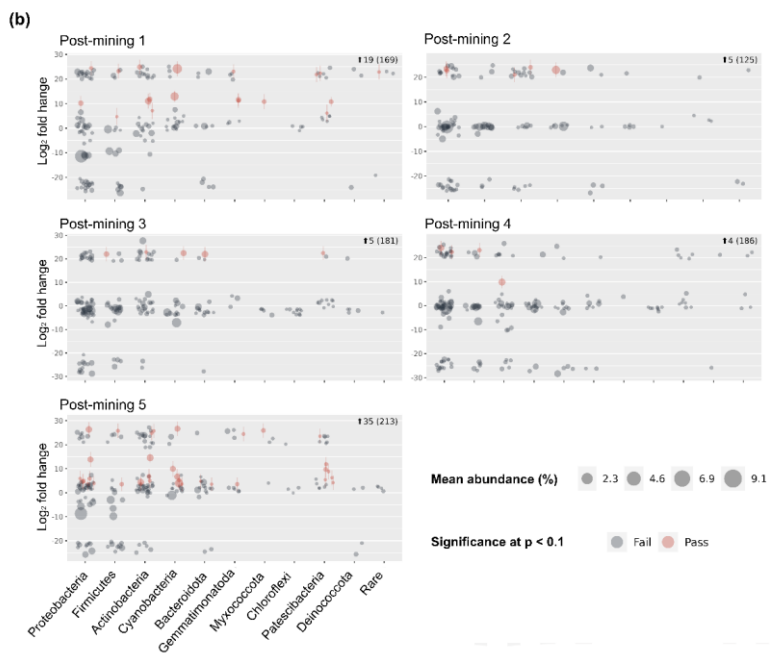
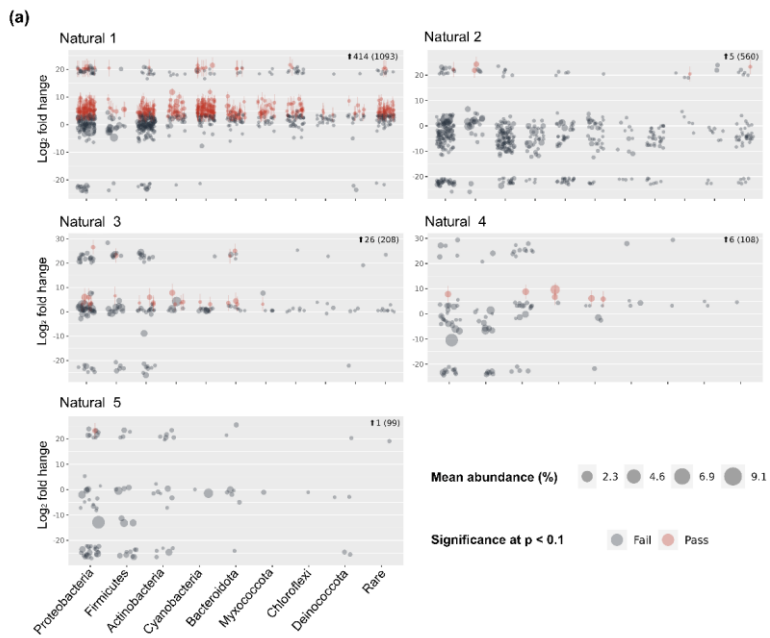
Formatted: Complex Script Font: Assistant Light

Formatted: Font: Italic, Complex Script Font: Italic

Formatted: Complex Script Font: Assistant Light

284 control, and the Log₂-fold change in labeled sequences was evaluated to determine whether
285 an ASV could be considered truly labeled (i.e., belonging to growing bacteria) based on the
286 significance threshold. One of the natural biocrust samples (no. 1; Fig. 4) displayed much
287 higher labeling than the other 4 samples (414 ASVs passed, out of a total of 1,093; Fig. 4).
288 Excluding sample 1, 38 out of 975 ASVs total passed the significance threshold for Log₂ fold
289 change. In post-mining samples, the number of labeled reads was more consistent among
290 the different samples (Fig. 4). 68 ASVs out of 874 ASVs total passed the threshold for Log₂ fold
291 change. Altogether, the number of labeled ASVs did not differ significantly between natural
292 and post-mining samples (natural sample 1 was excluded, natural community mean = 9.5,
293 post-mining community mean = 13.6, W= 9, p = 0.9).

294



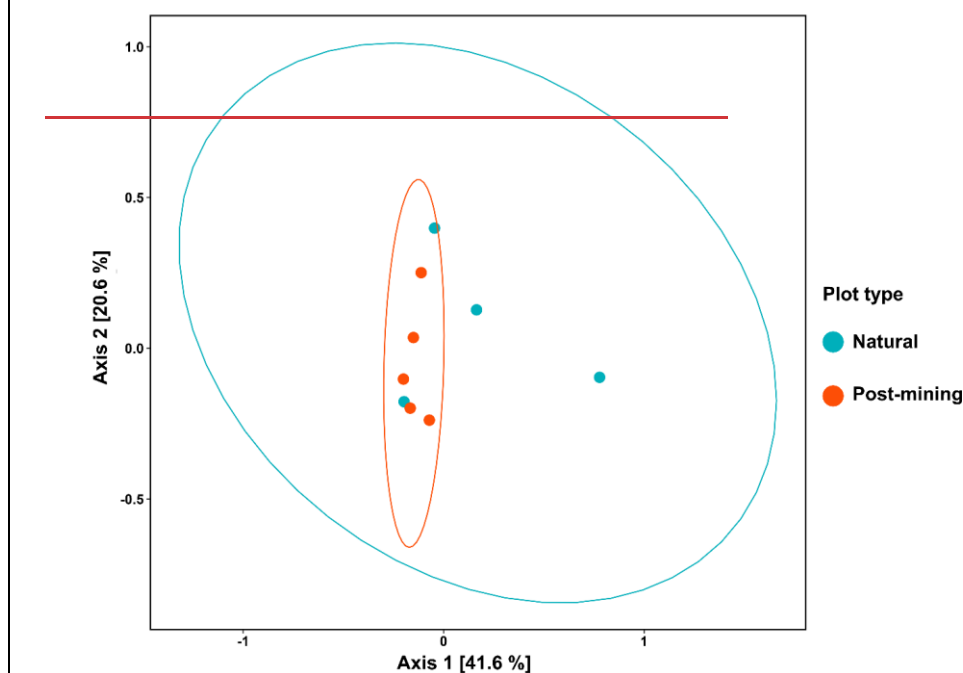
296 Figure 4: community composition of proliferated bacteria in natural (a) and post-mining (b)
297 biocrusts. Each graph represents a different sample. Red dots indicate labeled ASVs, and
298 grey dots indicate unlabeled ASVs, based on Deseq2 modeling.
299

300 **Composition of the proliferated bacterial community**

Formatted: Complex Script Font: Assistant Light

301 Figure 5(a) depicts a PCoA ordination based on weighted UniFrac metric showing that the
302 biocrust samples do not cluster according to plot type (natural sample number 1 was
303 excluded). Furthermore, the adonis test revealed no significant differences in community
304 composition (Weighted UniFrac ~ Plot type; $F = 1.23$, $R^2 = 0.15$, $p = 0.21$). A comparison of
305 phyla relative abundances reveals higher abundances of Cyanobacteria and Actinobacteria
306 in post-mining samples, and higher abundances of Firmicutes and Proteobacteria in natural
307 samples (Fig. 5(b)). However, none of the abundances differ significantly between groups
308 (Table S4). A Venn diagram of unique and overlapping sequences reveals that only 8 out of
309 88 labeled sequences appear both in natural and post-mining samples (Fig. S2). However,
310 Phylogenetic-phylogenetic trees depicting the different proliferated bacterial groups
311 indicating-indicate that, for the most part, sequences that appear in natural and post-mining
312 biocrusts belong to the same orders/classes. In the phylum Cyanobacteria, labeled
313 sequences belonged to two classes, and most sequences in both natural and post-mining
314 samples belonged to the class Cyanobacteria, with a slightly higher prevalence in the post-
315 mining samples (Fig. S1). The class Bacteroidia, belonging to the phylum Bacteroidota, had a
316 similar prevalence for natural and post-mining samples (Fig. S1). The trend was similar in the
317 class Bacilli, belonging to the phylum Firmicutes (Fig. S1). In the Alphaproteobacteria
318 phylum, the orders Rhodobacterales, Rhizobiales and Sphingomonadales appeared in both

319 natural and post-mining samples (Fig. S1). The phylum Gammaproteobacteria appeared
320 only once in post-mining samples but was more prevalent in natural samples (Fig. S1). The
321 phylum Actinobacteria was more prevalent in post-mining samples, yet the orders
322 Frankiales, Micrococcales and Propionibacteriales appeared in both natural and post-mining
323 samples (Fig. S1). A Venn diagram of unique and overlapping sequences reveals that only 8
324 out of 88 labeled sequences appear both in natural and post-mining samples (Fig. S2).



Formatted: Complex Script Font: Assistant Light

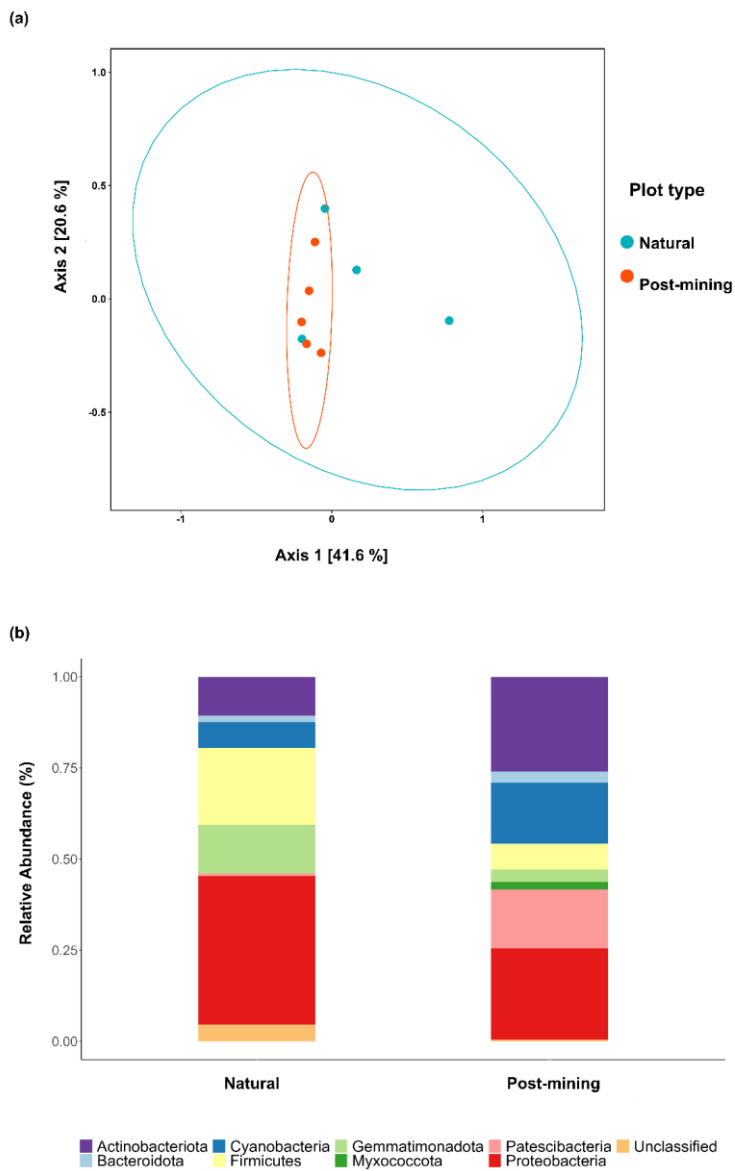


Figure 5: Composition of proliferated community. Top figure (a) depicts a PCoA ordination of community composition based on weighted UniFrac similarity metric. Blue dots are natural samples and pink dots are post-mining samples. The ellipses represent 95% confidence intervals-; the bottom figure (b) depicts a bar plot of phyla relative abundance (%) in natural and post-mining biocrusts.

332

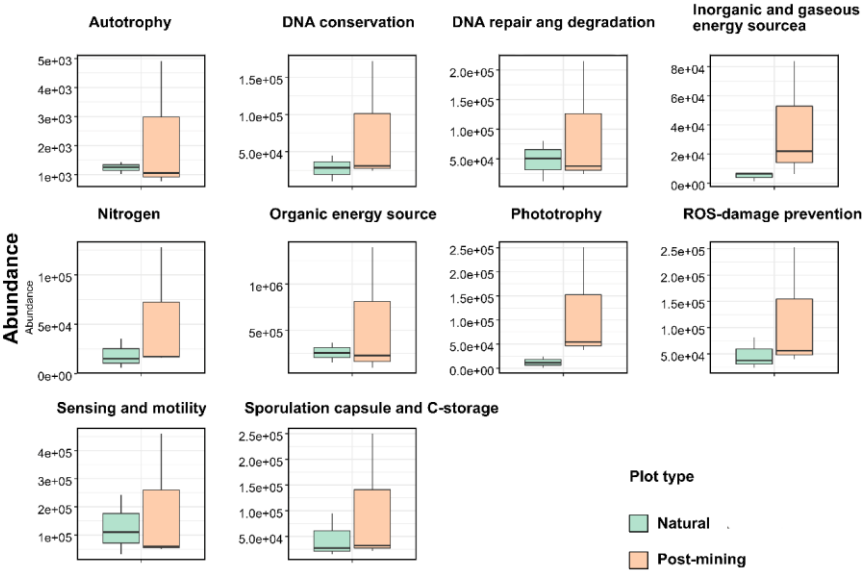
333 **Predictions of genomic functions**

Formatted: Complex Script Font: Assistant Light

334 Abundances of 10 function categories (listed in Table S4S5) were compared between natural
335 and post-mining biocrust samples. Abundances were generally higher in post-mining
336 compared to natural biocrusts (Fig. 6; Table S4S5). Also, the variance between samples was
337 larger in post-mining biocrust (Fig. 6). However, the differences between plot types were not
338 statistically significant in any of the function categories (Fig. 6; Table S4S5).

339

Formatted: Complex Script Font: Assistant Light



340 **Figure 6: boxplot of functional predictions.** The Y axis represents functional gene
341 abundances. The line represents the median, and the whiskers represent the range.

343

| 344

Formatted: Complex Script Font: Assistant Light

345 Discussion

346 In this study, we examined which groups of the biocrust bacterial communities grow after
347 hydration using a SIP assay and differential abundance [and diversity](#) modelling. We
348 hydrated and incubated the biocrusts for 96 hr expecting bacterial growth, yet very little
349 growth was detected. Only 3.9% of the natural and 7.7% of the post-mining biocrusts' ASVs
350 were identified as truly labeled by the stable isotope. Post-mining biocrusts had a slightly
351 higher number of labeled ASVs compared to natural biocrusts but, the differences were not
352 significant. Also, the composition and taxonomic identity of the growing communities did
353 not significantly differ between natural and post-mining biocrusts.

354
355 Biocrust organisms are known to resume activity quickly following hydration, resuming
356 functions such as damage repair, germination, nutrient cycling, and growth (Harel et al.,
357 2004, Rajeev et al., 2013, Green and Proctor, 2016, Thomas et al., 2022). Hydration [may was](#)
358 also [demonstrated to lead to](#) change [thes in](#) biocrust bacterial communities (Angel and
359 Conrad, 2013; Štovíček and Gillor, 2022). In a H₂¹⁸O SIP assay using the Negev Desert biocrusts
360 from arid and hyperarid regions, samples were hydrated and incubated for three weeks at
361 maximum water holding capacity. Within days, changes in the labeled bacterial community
362 composition and abundance were observed, indicating growth (Angel and Conrad, 2013).
363 Similarly, biocrusts collected in the Negev Desert [Highlands](#) during a rain event and
364 subsequent desiccation, demonstrated an increase in Cyanobacteria and decrease in

Formatted: Complex Script Font: Assistant Light

Formatted: Complex Script Font: Assistant Light

Formatted: Complex Script Font: Assistant Light

Formatted: Complex Script Font: Assistant Light

365 Actinobacteria ~~abundance~~ relative abundance (Baubin et al., 2021), implying selective
366 ~~proliferation activation~~ of bacterial taxa in the hydrated biocrust.

Formatted: Complex Script Font: Assistant Light

367
368 In other H₂¹⁸O SIP assays on soil bacterial communities, a quick response to re-wetting was
369 observed, and bacterial growth was evident within 24 to 72 hours of incubation (Blazewicz et
370 al., 2014, Aanderud et al., 2015). Thus, we assumed that hydration and incubation of

Formatted: Complex Script Font: Assistant Light

Formatted: Complex Script Font: Assistant Light

371 hyperarid biocrusts under favorable conditions would result in growth. Previous studies
372 examining the effect of a physical disturbance (repeated trampling) on biocrust
373 communities, revealed a decrease in the amount of extractable DNA, lower chlorophyll *a*,
374 and a decrease in biomass and cyanobacteria abundances (Kuske et al., 2012; Steven et al.,
375 2015; Chung et al., 2019). ~~We~~ However, these studies investigated a smaller scale localized
376 disturbance compared to a mining disturbance, where the biocrust is completely removed
377 over large spatial scales. Moreover, the previous studies were conducted in environments
378 that were, and climates that are less extreme than the hyper-arid Zin Valley. Therefore, thus,
379 we expected the effects on damage to the the biocrust in Zin post-mining sites to follow
380 similar patterns but to be equivalent more conspicuous than similar in nature the to but with
381 a greater effect than previously reported physical trampling disturbances biocrusts (Kuske
382 et al., 2012; Steven et al., 2015; Chung et al., 2019). ~~REFs. Our previous report results~~ (Gabay et
383 al., 2022) supported this notion; as we demonstrated differences in bacterial communities in
384 natural and post-mining biocrusts (Gabay et al., 2022). Thus, we expected expecting these
385 differences to be reflected in distinct the proliferated proliferating communities when
386 comparing of natural and to post-mining these biocrusts, given our previous results that

demonstrated that the bacterial community differed between natural and post-mining biocrusts (Gabay et al., 2022).

(Kuske et al., 2012; Steven et al., 2015; Chung et al., 2019) Our previous survey (2017) of biocrust bacterial communities in the Zin mining area, also revealed significantly lower abundances of cyanobacteria and chlorophyll *a* concentrations in post-mining biocrusts (Gabay et al., 2022). Out of the four mining sites surveyed, Gov (which was restored in 2007) showed the most considerable shift in biocrust community following mining. However, in the current study, we sampled post-mining biocrusts at a different location within the Gov mining site (~500 m away from the original plot) due to technical constraints. In the new location we found that the photosynthetic potential of the biocrust in the post-mining biocrust plots did not differ from the natural biocrust. These results highlight the importance of microenvironments in shaping the functionality of biocrusts (Garcia-Pichel and Belnap, 1996). The similarities in active communities and photosynthetic potential could be due to more developed biocrusts in the new sampling locations compared to the previous ones.

Photosynthetic activity is usually observed in biocrusts within minutes to hours after hydration by either dew or rain (Harel et al., 2004; Lange, 2003). In our experiment, we hydrated the biocrusts to capacity and then incubated the samples for 96 hr. During the incubation, most biocrust samples displayed some degree of greening, with more greening in the natural biocrusts (Fig. 2). This indicates that the photosynthetic bacteria in the

408 biocrust were activated upon wetting. Yet, no significant differences were detected between
 409 natural and post-mining biocrusts; chlorophyll *a* concentrations (Fig. 3) or abundances of
 410 photosynthesis related genes related to photosynthesis (Fig. 6). This implies that similar
 411 abundances of photosynthetic bacteria were activated upon wetting in both biocrusts, yet
 412 they barely proliferated (Fig. 4).
 413
 414 The PICRUSt analysis revealed no significant differences functional predictions in the
 415 abundances of genes within any of the function categories (examined (Fig. 6). A-In contrast, a
 416 previous study conducted in Avdat, the Negev Desert Highlands, examined the active
 417 bacterial communities during a hydration-rain- and subsequent desiccation-drying cycle
 418 (Baubin et al., 2021). The results indicated an increase in genes related to photosynthesis
 419 and, light, and sensing following hydration the rain, while the other function categories did
 420 not vary significantly (Baubin et al., 2021). We note that the identity and abundances of
 421 the functional genes in the dry biocrusts in this study detected by Baubin et al., (2021) and
 422 here (Fig. 6) are similar the abundances we observed. (Baubin et al., 2021). Therefore, we
 423 propose that that the lack of differences similarity between the post-mining and natural
 424 biocrust communities (Fig. 5) reflect similar functional potential between the post-mining
 425 and natural biocrusts (Fig. 6). However, the small number and low abundance of active ASVs
 426 were used to infer the abundances of functional genes (Fig. 6), and the large variance
 427 between samples in post-mining biocrusts could be masking significant differences (Table
 428 S5). This implies that similar abundances of photosynthetic bacteria were activated upon
 429 wetting in both biocrusts, yet, they barely proliferated (Fig. 4).

430

431 The growth patterns of biocrust organisms are affected by local environmental conditions
432 (Kim and Or, 2017). Zin mining fields are in ~~an~~ hyperarid region, where extreme heat events
433 are frequent in the summer, and rains are scarce and unpredicted. Moreover, in recent years
434 there were only two or three rain events during each rainy season (Zin factory meteorological
435 data). Hydration is the most important factor affecting biocrust organisms' growth rate while
436 long desiccation periods negatively affect growth (Zaady et al., 2016). Also, salinity levels in
437 Zin valley soils are high (Table 1; Levi et al., 2021) imposing further stress on the biocrust
438 community. It is known that in high stress environments, biocrust microorganisms increase
439 nutrient availability and accumulation by resumeing carbon and nitrogen fixation upon
440 hydration (Aranibar, 2022). The resulting organic carbon and nitrogen compounds can be
441 metabolized can be consumed during the long desiccation periods (Belnap, 2003; Colesie et
442 al., 2014). We suggest that due to these conditions, the hyperarid biocrust communities
443 prioritize activation and preparation for desiccation over growth. One study examining
444 microbial nitrogen transformations in biocrusts using collected from Succulent Karoo biome
445 in Namibia and South Africa showed that following wetting, nitrogen cycling genes are
446 expressed in biocrust organisms (Maier et al., 2022). while. Another study examining biocrust
447 samples taken from the Moab Desert in Utah demonstrated a pulse of metabolite release
448 following controlled wetting (Swenson et al., 2018). It is known that in high stress
449 environments, biocrust microorganisms resume carbon and nitrogen fixation upon
450 hydration. The resulting organic carbon and nitrogen compounds can be metabolized
451 during the long desiccation periods (Belnap, 2003; Colesie et al., 2014). Thus, bBased on

~~previous~~these reports, (~~Maier et al., 2022; Swenson et al., 2018~~) and due to the extreme conditions in Zin Valley- (Levi et al., 2021)(~~Levi et al., 2021~~), we suggest that ~~the~~ hyperarid biocrust communities prioritize functions such as metabolite production, nutrient cycling and preparation for desiccation over growth.

Natural recovery of biocrusts has been long debated, and is generally estimated to be a slow process, especially in [arid](#) sites that experience very short activity ~~times-periods~~ for biocrust development, such as the hyperarid Zin mining site (Kidron et al., 2020; Weber et al., 2016).

The time and trajectory of recovery depend on many factors relating to local climatic conditions and site properties (Belnap and Lange, 2003). One such factor that greatly affects establishment and restoration of biocrusts is the proximity, availability, and dispersal timing of biocrust propagules (Bowker, 2007; Walker et al., 2007)(~~Bowker, 2007; Walker et al., 2007~~).

Thus, the low proliferation rates we observed, particularly in post-mining biocrusts, suggest that restoration processes might be much slower than previously estimated. The topsoil from a stockpile is used to cover the mining pits. This soil may not contain a ~~rich~~ biocrust seed bank ~~that was~~[because it was](#) probably destroyed and buried during the mining processes. Further increase in bacterial biomass might highly depend on the dispersal of

biocrust propagules to the site from adjacent natural areas by wind or water. Our results further emphasize the need for active restoration measures in [the](#) Zin mines. Such measures include soil inoculation with local cyanobacterial propagules (~~Wang et al., 2009; Acea, 2003; Zhao et al., 2016; Velasco Ayuso et al., 2017~~)(~~Acea, 2003; Wang et al., 2009; Zhao et al., 2016; Velasco Ayuso et al., 2017~~) [Acea, 2003; Wang et al., 2009; Zhao et al., 2016; Velasco Ayuso et](#)

474 ~~al., 2017)~~ and increased hydration (Morillas and Gallardo, 2015; Zhang et al., 2018) (~~Morillas &~~
475 ~~Gallardo, 2015, Zhang et al., 2018)~~, which ~~are~~ were effective ~~methods~~ in enhancing biocrust
476 establishment and recovery following disturbances (Antoninka et al., 2020).

477
478

479 Conclusions

480 Low proliferation of biocrust bacteria was detected after wetting suggesting prolonged
481 recovery times of biocrusts following major mechanical disturbances, such as mining.
482 Furthermore, recovery largely depends on site conditions and the ability of biocrust
483 propagules to disperse to post-mining sites. Further research is needed to confirm our
484 hypothesis of low proliferation and thus restoration rates in hyper-arid biocrust bacterial
485 communities.

486

487 Code and data availability

488 All data produced in this study and scripts used for community analysis, functional
489 predictions and chlorophyll *a* estimation plot are available at
490 <https://github.com/TaliaJoanne/SIP-experiment-Zin-mines>.

491 The raw 16S sequences are available in the NCBI database under Bioproject ID
492 PRJNA906925, accession numbers SAMN31937891 – SAMN31937900.

493

Formatted: Complex Script Font: Assistant Light

Formatted: Complex Script Font: Assistant Light

Formatted: Complex Script Font: Assistant Light

Formatted: Complex Script Font: Assistant Light

Author's contributions

Talia Gabay: Conception, Sample Collection, Incubation, Chlorophyll *a* and DNA extraction, Statistical Analysis, Visualization, Writing-Original Draft Preparation, Writing-Reviewing and Editing. Eva Petrova: DNA-SIP assay, DNA quantification and PCR amplification. Osnat Gillor and Yaron Ziv: Conception, Writing-Reviewing and Editing, Investigation, Supervision. Roey Angel: Conception, Statistical Analysis, Visualization, Supervision, Writing-Reviewing and Editing.

All authors read and approved the manuscript.

Declaration of competing interest

The authors declare that they have no known competing financial interests or personal relationships that could have appeared to influence the work reported in this paper.

Acknowledgements

We thank Matan Avital from ICL for coordinating sample collection and providing Zin factory maps and meteorological data, Sharon Moscovitz for her assistance in sample collection and Ofer Ovadia for suggestions on statistical analyses. Lastly, we thank ICL Rotem LTD for their support and funding of this research.

Formatted: Complex Script Font: Assistant Light

Formatted: Complex Script Font: Assistant Light

513 **Financial support**

514 Funding for this research was provided by Rotem ICL LTD. RA was supported by the Czech
515 Science Foundation (Junior Grant No. 19-24309Y), EP was supported by the Czech Ministry of
516 Education Youth and Sport (EF16_013/0001782 - SoWa Ecosystems Research).

517

Formatted: Complex Script Font: Assistant Light

Formatted: Complex Script Font: Assistant Light

References

- Aanderud, Z. T., Jones, S. E., Fierer, N., and Lennon, J. T.: Resuscitation of the rare biosphere contributes to pulses of ecosystem activity, *Front. Microbiol.*, 6, <https://doi.org/10.3389/fmicb.2015.00024>, 2015.
- Acea, M.: Cyanobacterial inoculation of heated soils: effect on microorganisms of C and N cycles and on chemical composition in soil surface, *Soil Biology and Biochemistry*, 35, 513–524, [https://doi.org/10.1016/S0038-0717\(03\)00005-1](https://doi.org/10.1016/S0038-0717(03)00005-1), 2003.
- Angel, R.: Stable Isotope Probing Techniques and Methodological Considerations Using $\text{^{15}N}$, in: *Stable Isotope Probing: Methods and Protocols*, edited by: Dumont, M. G. and Hernández García, M., Springer New York, New York, NY, 175–187, https://doi.org/10.1007/978-1-4939-9721-3_14, 2019.
- Angel, R. and Conrad, R.: Elucidating the microbial resuscitation cascade in biological soil crusts following a simulated rain event: Microbial resuscitation in biological soil crusts, *Environ Microbiol*, n/a-n/a, <https://doi.org/10.1111/1462-2920.12140>, 2013.
- Angel, R., Panhölzl, C., Gabriel, R., Herbold, C., Wanek, W., Richter, A., Eichorst, S. A., and Woebken, D.: Application of stable-isotope labelling techniques for the detection of active diazotrophs: Detecting diazotrophs with stable-isotope techniques, *Environ Microbiol*, 20, 44–61, <https://doi.org/10.1111/1462-2920.13954>, 2018.
- Anon: Dabestr: Data Analysis Using Bootstrap-Coupled Estimation, 2020.
- Antoninka, A., Faist, A., Rodriguez-Caballero, E., Young, K. E., Chaudhary, V. B., Condon, L. A., and Pyke, D. A.: Biological soil crusts in ecological restoration: emerging research and perspectives, *Restor Ecol*, 28, <https://doi.org/10.1111/rec.13201>, 2020.
- Apprill, A., McNally, S., Parsons, R., and Weber, L.: Minor revision to V4 region SSU rRNA 806R gene primer greatly increases detection of SAR11 bacterioplankton, *Aquat. Microb. Ecol.*, 75, 129–137, <https://doi.org/10.3354/ame01753>, 2015.
- Aranibar, J. N.: Functional responses of biological soil crusts to simulated small precipitation pulses in the Monte desert, Argentina, 2022.
- Arslan, M., Müller, J. A., and Gamal El-Din, M.: Aerobic naphthenic acid-degrading bacteria in petroleum-coke improve oil sands process water remediation in biofilters: DNA-stable isotope probing reveals methylotrophy in Schmutzdecke, *Science of The Total Environment*, 815, 151961, <https://doi.org/10.1016/j.scitotenv.2021.151961>, 2022.
- Baubin, C., Ran, N., Siebner, H., and Gillor, O.: The response of desert biocrust bacterial communities to hydration-desiccation cycles, *SOIL Discussions*, 1–48, 2021.
- Belnap, J.: The world at your feet: desert biological soil crusts, *Frontiers in Ecology and the Environment*, 1, 181–189, [https://doi.org/10.1890/1540-9295\(2003\)001\[0181:TWAYFD\]2.0.CO;2](https://doi.org/10.1890/1540-9295(2003)001[0181:TWAYFD]2.0.CO;2), 2003.

Formatted: Font: (Default) Assistant Light, 14 pt,
Complex Script Font: Assistant Light, 14 pt

Formatted: Font: 11 pt, Complex Script Font: Assistant
Light, 11 pt

553 Belnap, J. and Eldridge, D.: Disturbance and Recovery of Biological Soil Crusts, in: Biological Soil
554 Crusts: Structure, Function, and Management, edited by: Belnap, J. and Lange, O. L., Springer Berlin
555 Heidelberg, Berlin, Heidelberg, 363–383, https://doi.org/10.1007/978-3-642-56475-8_27, 2003.

556 Belnap, J. and Lange, O. L. (Eds.) Baldwin, I. T., Caldwell, M. M., Heldmaier, G., Lange, O. L., Mooney, H.
557 A., Schulze, E.-D., and Sommer, U.: Biological Soil Crusts: Structure, Function, and Management,
558 Springer Berlin Heidelberg, Berlin, Heidelberg, <https://doi.org/10.1007/978-3-642-56475-8>, 2003.

559 Blazewicz, S. J., Schwartz, E., and Firestone, M. K.: Growth and death of bacteria and fungi underlie
560 rainfall-induced carbon dioxide pulses from seasonally dried soil, *Ecology*, 95, 1162–1172,
561 <https://doi.org/10.1890/13-1031.1>, 2014.

562 Blazewicz, S. J., Hungate, B. A., Koch, B. J., Nuccio, E. E., Morrissey, E., Brodie, E. L., Schwartz, E., Pett-
563 Ridge, J., and Firestone, M. K.: Taxon-specific microbial growth and mortality patterns reveal distinct
564 temporal population responses to rewetting in a California grassland soil, *ISME J*, 14, 1520–1532,
565 <https://doi.org/10.1038/s41396-020-0617-3>, 2020.

566 Bowker, M. A.: Biological Soil Crust Rehabilitation in Theory and Practice: An Underexploited
567 Opportunity, *Restor Ecology*, 15, 13–23, <https://doi.org/10.1111/j.1526-100X.2006.00185.x>, 2007.

568 Bridge, G.: CONTESTED TERRAIN: Mining and the Environment, *Annu. Rev. Environ. Resour.*, 29, 205–
569 259, <https://doi.org/10.1146/annurev.energy.28.011503.163434>, 2004.

570 Callahan, B. J., McMurdie, P. J., Rosen, M. J., Han, A. W., Johnson, A. J. A., and Holmes, S. P.: DADA2:
571 High-resolution sample inference from Illumina amplicon data, *Nat Methods*, 13, 581–583,
572 <https://doi.org/10.1038/nmeth.3869>, 2016.

573 Chung, Y. A., Thornton, B., Dettweiler-Robinson, E., and Rudgers, J. A.: Soil surface disturbance alters
574 cyanobacterial biocrusts and soil properties in dry grassland and shrubland ecosystems, *Plant Soil*,
575 441, 147–159, <https://doi.org/10.1007/s11104-019-04102-0>, 2019.

576 Colesie, C., Allan Green, T. G., Haferkamp, I., and Büdel, B.: Habitat stress initiates changes in
577 composition, CO₂ gas exchange and C-allocation as life traits in biological soil crusts, *ISME J*, 8, 2104–
578 2115, <https://doi.org/10.1038/ismej.2014.47>, 2014.

579 Davis, N. M., Proctor, D., Holmes, S. P., Relman, D. A., and Callahan, B. J.: Simple statistical
580 identification and removal of contaminant sequences in marker-gene and metagenomics data,
581 *bioRxiv*, 221499, <https://doi.org/10.1101/221499>, 2017.

582 Dixon, P.: VEGAN, a package of R functions for community ecology, *Journal of Vegetation Science*, 14,
583 927–930, <https://doi.org/10.1111/j.1654-1103.2003.tb02228.x>, 2003.

584 Douglas, G. M., Maffei, V. J., Zaneveld, J., Yurgel, S. N., Brown, J. R., Taylor, C. M., Huttenhower, C., and
585 Langille, M. G. I.: PICRUSt2: An improved and customizable approach for metagenome inference,
586 *Bioinformatics*, <https://doi.org/10.1101/672295>, 2019.

587 Dumont, M. G. and Hernández García, M. (Eds.): Stable Isotope Probing: Methods and Protocols,
588 Springer New York, New York, NY, <https://doi.org/10.1007/978-1-4939-9721-3>, 2019.

589 Gabay, T., Rotem, G., Gillor, O., and Ziv, Y.: Understanding changes in biocrust communities following
590 phosphate mining in the Negev Desert, *Environmental Research*, 207, 112200,
591 <https://doi.org/10.1016/j.envres.2021.112200>, 2022.

592 Garcia-Pichel, F. and Belnap, J.: Microenvironments and Microscale Productivity of Cyanobacterial
593 Desert Crusts, *J Phycol*, 32, 774–782, <https://doi.org/10.1111/j.0022-3646.1996.00774.x>, 1996.

594 Green, T. G. A. and Proctor, M. C. F.: Physiology of Photosynthetic Organisms Within Biological Soil
595 Crusts: Their Adaptation, Flexibility, and Plasticity, in: *Biological Soil Crusts: An Organizing Principle in*
596 *Drylands*, edited by: Weber, B., Büdel, B., and Belnap, J., Springer International Publishing, Cham,
597 347–381, https://doi.org/10.1007/978-3-319-30214-0_18, 2016.

598 Harel, Y., Ohad, I., and Kaplan, A.: Activation of Photosynthesis and Resistance to Photoinhibition in
599 Cyanobacteria within Biological Desert Crust, *Plant Physiology*, 136, 3070–3079,
600 <https://doi.org/10.1104/pp.104.047712>, 2004.

601 Jia, Z., Cao, W., and Hernández García, M.: DNA-based stable isotope probing, in: *Stable Isotope*
602 *Probing*, Springer, 17–29, 2019.

603 Kidron, G. J., Xiao, B., and Benenson, I.: Data variability or paradigm shift? Slow versus fast recovery of
604 biological soil crusts-a review, *Science of The Total Environment*, 721, 137683,
605 <https://doi.org/10.1016/j.scitotenv.2020.137683>, 2020.

606 Kim, M. and Or, D.: Hydration status and diurnal trophic interactions shape microbial community
607 function in desert biocrusts, *Biogeosciences*, 14, 5403–5424, <https://doi.org/10.5194/bg-14-5403-2017>,
608 2017.

609 Kuske, C. R., Yeager, C. M., Johnson, S., Ticknor, L. O., and Belnap, J.: Response and resilience of soil
610 biocrust bacterial communities to chronic physical disturbance in arid shrublands, *ISME J*, 6, 886–
611 897, <https://doi.org/10.1038/ismej.2011.153>, 2012.

612 Lange, O. L.: Photosynthesis of Soil-Crust Biota as Dependent on Environmental Factors, in:
613 *Biological Soil Crusts: Structure, Function, and Management*, edited by: Belnap, J. and Lange, O. L.,
614 Springer Berlin Heidelberg, Berlin, Heidelberg, 217–240, [https://doi.org/10.1007/978-3-642-56475-](https://doi.org/10.1007/978-3-642-56475-8_18)
615 [8_18](https://doi.org/10.1007/978-3-642-56475-8_18), 2003.

616 Levi, N., Hillel, N., Zaady, E., Rotem, G., Ziv, Y., Karnieli, A., and Paz-Kagan, T.: Soil quality index for
617 assessing phosphate mining restoration in a hyper-arid environment, *Ecological Indicators*, 125,
618 107571, <https://doi.org/10.1016/j.ecolind.2021.107571>, 2021.

619 Love, M. I., Huber, W., and Anders, S.: Moderated estimation of fold change and dispersion for RNA-
620 seq data with DESeq2, *Genome Biol*, 15, 550, <https://doi.org/10.1186/s13059-014-0550-8>, 2014.

621 Lozupone, C., Lladser, M. E., Knights, D., Stombaugh, J., and Knight, R.: UniFrac: an effective distance
622 metric for microbial community comparison, *The ISME journal*, 5, 169–172, 2011.

623 Macey, M. C., Pratscher, J., Crombie, A. T., and Murrell, J. C.: Impact of plants on the diversity and
624 activity of methylotrophs in soil, *Microbiome*, 8, 31, <https://doi.org/10.1186/s40168-020-00801-4>, 2020.

625 Maier, S., Kratz, A. M., Weber, J., Prass, M., Liu, F., Clark, A. T., Abed, R. M. M., Su, H., Cheng, Y.,
626 Eickhorst, T., Fiedler, S., Pöschl, U., and Weber, B.: Water-driven microbial nitrogen transformations in
627 biological soil crusts causing atmospheric nitrous acid and nitric oxide emissions, *ISME J*, 16, 1012–
628 1024, <https://doi.org/10.1038/s41396-021-01127-1>, 2022.

629 Makhalanyane, T. P., Valverde, A., Gunnigle, E., Frossard, A., Ramond, J.-B., and Cowan, D. A.:
630 Microbial ecology of hot desert edaphic systems, *FEMS Microbiology Reviews*, 39, 203–221,
631 <https://doi.org/10.1093/femsre/fuu011>, 2015.

632 McMurdie, P. J. and Holmes, S.: phyloseq: An R Package for Reproducible Interactive Analysis and
633 Graphics of Microbiome Census Data, *PLOS ONE*, 8, e61217,
634 <https://doi.org/10.1371/journal.pone.0061217>, 2013.

635 Meier, D. V., Imminger, S., Gillor, O., and Woebken, D.: Distribution of Mixotrophy and Desiccation
636 Survival Mechanisms across Microbial Genomes in an Arid Biological Soil Crust Community,
637 *mSystems*, 6, e00786–20, <https://doi.org/10.1128/mSystems.00786-20>, 2021.

638 Minh, B. Q., Schmidt, H. A., Chernomor, O., Schrempf, D., Woodhams, M. D., von Haeseler, A., and
639 Lanfear, R.: IQ-TREE 2: New Models and Efficient Methods for Phylogenetic Inference in the Genomic
640 Era, *Molecular Biology and Evolution*, 37, 1530–1534, <https://doi.org/10.1093/molbev/msaa015>, 2020.

641 Morillas, L. and Gallardo, A.: Biological soil crusts and wetting events: Effects on soil N and C cycles,
642 *Applied Soil Ecology*, 94, 1–6, <https://doi.org/10.1016/j.apsoil.2015.04.015>, 2015.

643 Parada, A. E., Needham, D. M., and Fuhrman, J. A.: Every base matters: assessing small subunit rRNA
644 primers for marine microbiomes with mock communities, time series and global field samples,
645 *Environmental microbiology*, 18, 1403–1414, 2016.

646 Pepe-Ranney, C., Koechli, C., Potrafka, R., Andam, C., Eggleston, E., Garcia-Pichel, F., and Buckley, D.
647 H.: Non-cyanobacterial diazotrophs mediate dinitrogen fixation in biological soil crusts during early
648 crust formation, *ISME J*, 10, 287–298, <https://doi.org/10.1038/ismej.2015.106>, 2016.

649 Rajeev, L., da Rocha, U. N., Klitgord, N., Luning, E. G., Fortney, J., Axen, S. D., Shih, P. M., Bouskill, N. J.,
650 Bowen, B. P., Kerfeld, C. A., Garcia-Pichel, F., Brodie, E. L., Northen, T. R., and Mukhopadhyay, A.:
651 Dynamic cyanobacterial response to hydration and dehydration in a desert biological soil crust, *ISME*
652 *J*, 7, 2178–2191, <https://doi.org/10.1038/ismej.2013.83>, 2013.

653 Ritchie, R. J.: Consistent Sets of Spectrophotometric Chlorophyll Equations for Acetone, Methanol
654 and Ethanol Solvents, *Photosynth Res*, 89, 27–41, <https://doi.org/10.1007/s11120-006-9065-9>, 2006.

655 Schwartz, E., Hayer, M., Hungate, B. A., and Mau, R. L.: Stable Isotope Probing of Microorganisms in
656 Environmental Samples with H 2 18 O, in: *Stable Isotope Probing*, Springer, 129–136, 2019.

657 Sengupta, M.: Environmental impacts of mining: monitoring, restoration, and control, Second
658 edition., CRC Press, Boca Raton, FL ; Abingdon, Oxon, 1 pp., 2021.

659 Steven, B., Kuske, C. R., Gallegos-Graves, L. V., Reed, S. C., and Belnap, J.: Climate Change and
660 Physical Disturbance Manipulations Result in Distinct Biological Soil Crust Communities, *Appl*
661 *Environ Microbiol*, 81, 7448–7459, <https://doi.org/10.1128/AEM.01443-15>, 2015.

662 Štovíček, A. and Gillor, O.: The Response of Soil Microbial Communities to Hydration and Desiccation
663 Cycles in Hot Desert Ecosystems, in: *Microbiology of Hot Deserts*, edited by: Ramond, J.-B. and
664 Cowan, D. A., Springer International Publishing, Cham, 319–339, [https://doi.org/10.1007/978-3-030-](https://doi.org/10.1007/978-3-030-98415-1_11)
665 [98415-1_11](https://doi.org/10.1007/978-3-030-98415-1_11), 2022.

666 Sultana, N., Zhao, J., Zheng, Y., Cai, Y., Faheem, M., Peng, X., Wang, W., and Jia, Z.: Stable isotope
667 probing of active methane oxidizers in rice field soils from cold regions, *Biol Fertil Soils*, 55, 243–250,
668 <https://doi.org/10.1007/s00374-018-01334-7>, 2019.

669 Swenson, T. L., Karaoz, U., Swenson, J. M., Bowen, B. P., and Northen, T. R.: Linking soil biology and
670 chemistry in biological soil crust using isolate exometabolomics, *Nat Commun*, 9, 19,
671 <https://doi.org/10.1038/s41467-017-02356-9>, 2018.

672 Team, R. C.: *R: A language and environment for statistical computing*, 2013.

673 Thomas, A. D., Elliott, D. R., Hardcastle, D., Strong, C. L., Bullard, J., Webster, R., and Lan, S.: Soil
674 biocrusts affect metabolic response to hydration on dunes in west Queensland, Australia, *Geoderma*,
675 405, 115464, <https://doi.org/10.1016/j.geoderma.2021.115464>, 2022.

676 Velasco Ayuso, S., Giraldo Silva, A., Nelson, C., Barger, N. N., and Garcia-Pichel, F.: Microbial Nursery
677 Production of High-Quality Biological Soil Crust Biomass for Restoration of Degraded Dryland Soils,
678 *Appl Environ Microbiol*, 83, e02179-16, <https://doi.org/10.1128/AEM.02179-16>, 2017.

679 Walker, L. R., Walker, J., and Hobbs, R. J. (Eds.): *Linking restoration and ecological succession*,
680 Springer, New York, NY, 190 pp., 2007.

681 Wang, W., Liu, Y., Li, D., Hu, C., and Rao, B.: Feasibility of cyanobacterial inoculation for biological soil
682 crusts formation in desert area, *Soil Biology and Biochemistry*, 41, 926–929,
683 <https://doi.org/10.1016/j.soilbio.2008.07.001>, 2009.

684 Weber, B., Büdel, B., and Belnap, J. (Eds.): *Biological Soil Crusts: An Organizing Principle in Drylands*,
685 Springer International Publishing, Cham, <https://doi.org/10.1007/978-3-319-30214-0>, 2016.

686 Weber, B., Belnap, J., Büdel, B., Antoninka, A. J., Barger, N. N., Chaudhary, V. B., Darrouzet-Nardi, A.,
687 Eldridge, D. J., Faist, A. M., Ferrenberg, S., Havrilla, C. A., Huber-Sannwald, E., Malam Issa, O., Maestre,
688 F. T., Reed, S. C., Rodriguez-Caballero, E., Tucker, C., Young, K. E., Zhang, Y., Zhao, Y., Zhou, X., and
689 Bowker, M. A.: What is a biocrust? A refined, contemporary definition for a broadening research
690 community, *Biological Reviews*, 97, 1768–1785, <https://doi.org/10.1111/brv.12862>, 2022.

691 Yu, Y., Lee, C., Kim, J., and Hwang, S.: Group-specific primer and probe sets to detect methanogenic
692 communities using quantitative real-time polymerase chain reaction, *Biotechnology and*
693 *bioengineering*, 89, 670–679, 2005.

694 Zaady, E., Eldridge, D. J., and Bowker, M. A.: Effects of Local-Scale Disturbance on Biocrusts, in:
695 *Biological Soil Crusts: An Organizing Principle in Drylands*, edited by: Weber, B., Büdel, B., and Belnap,
696 J., Springer International Publishing, Cham, 429–449, https://doi.org/10.1007/978-3-319-30214-0_21,
697 2016.

698 Zhang, C., Niu, D., Song, M., Elser, J. J., Okie, J. G., and Fu, H.: Effects of rainfall manipulations on
699 carbon exchange of cyanobacteria and moss-dominated biological soil crusts, *Soil Biology and*
700 *Biochemistry*, 124, 24–31, <https://doi.org/10.1016/j.soilbio.2018.05.021>, 2018.

701 Zhang, L., Dumont, M. G., Bodelier, P. L. E., Adams, J. M., He, D., and Chu, H.: DNA stable-isotope
702 probing highlights the effects of temperature on functionally active methanotrophs in natural
703 wetlands, *Soil Biology and Biochemistry*, 149, 107954, <https://doi.org/10.1016/j.soilbio.2020.107954>,
704 2020.

705 Zhao, Y., Bowker, M. A., Zhang, Y., and Zaady, E.: Enhanced Recovery of Biological Soil Crusts After
706 Disturbance, in: *Biological Soil Crusts: An Organizing Principle in Drylands*, vol. 226, edited by: Weber,
707 B., Büdel, B., and Belnap, J., Springer International Publishing, Cham, 499–523,
708 https://doi.org/10.1007/978-3-319-30214-0_24, 2016.

709 ▲

Formatted: Complex Script Font: Assistant Light